A Generic Approach for the Purification of Signaling Complexes That Specifically Interact with the Carboxyl-terminal Domain of G Protein-coupled Receptors

Pascal Maurice, Avais M Daulat, Cédric Broussard, Julien Mozo, Guilhem Clary, Françoise Hotellier, Philippe Chafey, Jean-Luc Guillaume, Gilles Ferry, Jean A. Boutin, et al.

A Generic Approach for the Purification of Signaling Complexes That Specifically Interact with the Carboxyl-terminal Domain of G Protein-coupled Receptors*[S]

Pascal Maurice‡§, Avais M. Daulat‡§¶, Cédric Broussard§‖, Julien Mozo, Guilhem Clary§‖, Françoise Hotellier§‖, Philippe Chafey§‖, Jean-Luc Guillaume‡§, Gilles Ferry**, Jean A. Boutin**, Philippe Delagrange**, Luc Camoin§‖, and Ralf Jockers‡§‡‡**

G protein-coupled receptors (GPCRs) constitute the largest family of membrane receptors and are major drug targets. Recent progress has shown that GPCRs are part of large protein complexes that regulate their activity. We present here a generic approach for identification of these complexes that is based on the use of receptor subdomains and that overcomes the limitations of currently used genetics and proteomics approaches. Our approach consists of a carefully balanced combination of chemically synthesized His_6-tagged baits, immobilized metal affinity chromatography, one- and two-dimensional gel electrophoresis separation and mass spectrometric identification. The carboxyl-terminal tails (C-tails) of the human MT_1 and MT_2 melatonin receptors, two class A GPCRs, were used as models to purify protein complexes from mouse brain lysates. We identified 32 proteins that interacted with the C-tail of MT_1, 14 proteins that interacted with the C-tail of MT_2, and eight proteins that interacted with both C-tails. Several randomly selected proteins were validated by Western blotting, and the functional relevance of our data was further confirmed by showing the interaction between the full-length MT_1 and the regulator of G protein signaling Z1 in transfected HEK 293 cells and native tissue. Taken together, we have established an integrated and generic purification strategy for the identification of high quality and functionally relevant GPCR-associated protein complexes that significantly widens the repertoire of available techniques. ***Molecular & Cellular Proteomics 7: 1556–1569, 2008.***

G protein-coupled receptors (GPCRs)[1] constitute the largest family of membrane receptors with more than 800 members (1, 2). By binding to a great variety of ligands (photons, odorants, amino acids, nucleotides, peptides, proteins, and lipids), GPCRs are key receptors of numerous physiological processes such as neurotransmission, cell metabolism, secretion, cell differentiation, and growth and are targeted by about half of the drugs prescribed for human diseases (3). It is now well established that GPCRs do not only couple to heterotrimeric G proteins but can also physically associate with other less well known intracellular proteins regulating receptor trafficking, subcellular localization, signaling, and desensitization (4, 5). Intracellular proteins can interact directly or indirectly, via adaptor proteins, with intracellular receptor domains. Among these domains, the carboxyl-terminal tail (C-tail) is considered a key domain able to recruit intracellular proteins in large submembrane signaling networks (6, 7).

Several approaches have been described in the literature to identify proteins that interact with GPCRs. The yeast two-hybrid assay has been used to screen for proteins that bind to cytosolic domains of GPCRs (8–10). However, this system, which is very sensitive for the detection of *in vivo* protein-protein interactions, has shown several limitations including the generation of many false positives and negatives, the detection of only binary interactions, and the non-physiological relevance of the identified interactions (*e.g.* occurring in the yeast nucleus). Moreover this approach is not designed to

From the ‡Department of Cell Biology and ‖Laboratoire de Protéomique, Institut Cochin, Université Paris Descartes, CNRS (UMR 8104), Paris F-75014, France, §INSERM U567, Paris F-75014, France, and **Institut de Recherches SERVIER, Suresnes F-92150, France

Received, September 12, 2007, and in revised form, April 28, 2008
Published, MCP Papers in Press, April 29, 2008, DOI 10.1074/mcp.M700435-MCP200

[1] The abbreviations used are: GPCR, G protein-coupled receptor; C-tail, carboxyl-terminal tail; 1D, one-dimensional; 2D, two-dimensional; Ni-NTA, nickel-nitrilotriacetic acid; MT, melatonin receptor; PDZ, PSD-95/Disc-large/ZO-1; ERK, extracellular signal-regulated kinase; CK2, casein kinase II; GRK, G protein-coupled receptor kinase; HEK, human embryonic kidney; 5-HT, 5-hydroxytryptamine; RGSZ1, regulator of G protein signaling Z1; ABC, ammonium bicarbonate; nNOS, neuronal NO synthase; PKC, protein kinase C; HA, hemagglutinin; GTPγS, guanosine 5′-3-O-(thio)triphosphate; CHO, Chinese hamster ovary; RGS, regulator of G protein signaling; YFP, yellow fluorescent protein; PSD, postsynaptic density; TAP, tandem affinity purification.

identify protein complexes. To overcome these limitations, proteomics approaches were developed based on peptide affinity chromatography coupled to protein identification by mass spectrometry. The first generation used the entire receptor C-tail expressed as a GST fusion protein in *Escherichia coli* to purify the interactome of the C-tail from brain lysates (11). Although some interacting proteins have been identified for the 5-HT_{2C} receptor, several limitations prevented a more general application of this approach. Indeed the amount of nonspecifically retained proteins is high because of the presence of contaminating bacterial proteins, full-length and truncated GST fusion proteins, and proteins that nonspecifically bind to the GST carrier. In addition, the complex sample has to be separated by two-dimensional (2D) electrophoresis before mass spectrometry analysis of the recruited proteins, thus minimizing the number of potential candidates because of the limitations inherent to 2D electrophoresis for hydrophobic, basic, and large proteins. The second generation of peptide affinity chromatography is based on the use of short synthetic peptides encompassing a specific interaction motif that recruit only the proteins that interact with this specific motif. The amount of nonspecific proteins is indeed largely reduced in this approach, and the pattern of specific interaction partners is much less complex. Consequently this approach has been successfully used for several GPCRs and is expected to be applied to multiple GPCR interaction motifs (12, 13). However, this evolution of peptide affinity chromatography does not respond to the initial task, the identification of the interactome of the entire C-tail, without prior knowledge of specific interaction motifs.

In the present study, we present an improved peptide affinity chromatography that has the potential to become the first generic approach for the purification of GPCR C-tail-associated protein complexes. We combined the use of chemically synthesized His_6-tagged peptides encompassing the entire receptor C-tail combined with metal affinity immobilization on a Ni-NTA matrix to recover protein complexes from mouse brain lysates. The C-tails of the MT_1 and MT_2 melatonin receptors, typical class A GPCRs, were used as model receptors. Major features of this approach are the low nonspecific binding, the high integrity of recovered complexes, and the compatibility with 1D and 2D electrophoresis. We report the identification of 40 and 22 proteins that specifically associate with the C-tails of MT_1 and MT_2, respectively. To demonstrate the functional relevance of the identified protein complexes, we selected the interaction between MT_1 and the regulator of G protein signaling Z1 (RGSZ1) for further characterization in transfected HEK 293 cells and native tissue.

EXPERIMENTAL PROCEDURES

Peptide Affinity Chromatography—Peptides encompassing the C-tails of the MT_1 and MT_2 receptors were chemically synthesized by NeoMPS (Strasbourg, France) with a His_6 tag at the amino terminus. The synthetic peptides (MT_1, last 61 amino acids, 7.16 kDa, 88.5% purity; MT_2, last 58 amino acids, 6.80 kDa, 90% purity) were coupled via the His_6 tag to Ni-NTA-agarose beads (Qiagen).

Brains of C57/Bl6 mice were crushed in 20 ml of buffer containing 20 mM NaH_2PO_4, 2 mM Na_3VO_4, 10 mM NaF, protease inhibitor mixture EDTA-free (Roche Applied Science), pH 8.0, using an Ultra-Turrax T25 (Janke-Kunkel). CHAPS (10 mM final concentration) and NaCl (150 mM final concentration) were added, and the homogenates were incubated for 3 h at 4 °C under gentle end-over-end mixing. After centrifugation (10,000 × *g* for 1 h at 4 °C), the supernatants were collected, and the protein concentration was determined by BCA assay (Pierce).

Supernatants (10 mg of solubilized brain proteins) were incubated overnight at 4 °C with 20 μl of Ni-NTA-agarose beads (300–350 μg of immobilized peptide) in the presence of 20 mM imidazole to reduce nonspecific binding. The beads were washed five times in washing buffer (20 mM NaH_2PO_4, 2 mM Na_3VO_4, 10 mM NaF, protease inhibitor mixture EDTA-free, 10 mM CHAPS, 150 mM NaCl, 20 mM imidazole, pH 8), and proteins retained by affinity were eluted with either 50 μl of 2% SDS in PBS (95 °C for 10 min) for BCA measurements, 1D electrophoresis, and immunoblotting or 200 μl of rehydration buffer (8 M urea, 2 M thiourea, 4% CHAPS) for 45 min at room temperature for 2D electrophoresis.

1D and 2D Electrophoresis—For 1D electrophoresis, eluted proteins with 2% SDS in PBS were denatured in SDS-PAGE loading buffer (62.5 mM Tris/HCl, pH 6.8, 2% SDS, 10% glycerol, 0.5% bromphenol blue) for 5 min at 95 °C. Samples were subjected to SDS-PAGE on a 10 or 5–9% gradient polyacrylamide gel, and proteins were silver-stained according to Rabilloud and Charmont (14).

For 2D electrophoresis, eluted proteins in rehydration buffer were first separated according to their isoelectric point along a nonlinear IPG strip (pH 3–11 nonlinear, 11 cm long) using the IPGphor apparatus (GE Healthcare). DeStreack Reagent (15 mg/ml of rehydration solution; GE Healthcare) and ampholytes (1% IPG buffer; GE Healthcare) were added to the sample, and then sample loading for the first dimension was performed by passive in-gel rehydration. Focalization was stopped when 27,000 V-h were reached. After the first dimension, the IPG strips were equilibrated for 15 min in buffer A (6 M urea, 2% SDS, 30% glycerol, 50 mM Tris/HCl, pH 8.6) containing 1% DTT and then for 15 min in buffer A containing 4.7% iodoacetamide. For the second dimension, the strips were loaded on 8–18% SDS-polyacrylamide gels. The gels were then silver-stained according to Rabilloud and Charmont (14).

In-gel Trypsin Digestion—Spots of interest were excised from the gel, washed with 200 mM ammonium bicarbonate (ABC) and immediately destained according to Gharahdaghi *et al.* (15). In-gel trypsin digestion was carried out as described in a protocol based on the ZipTip Plate (Millipore) with minor modifications. After destaining, spots were rinsed three times with water and shrunk with 50 mM ABC, 50% ACN for 20 min at room temperature. Gel pieces were dried using 100% ACN for 15 min and then incubated in 50 mM ABC containing 10 mM DTT for 1 h at 56 °C. The solution was then replaced by 55 mM iodoacetamide in 50 mM ABC for 30 min in the dark at room temperature. The gel pieces were washed twice with 50 mM ABC, finally shrunk with 25 mM ABC, 50% ACN for 30 min, and dried using 100% ACN for 10 min. Gel pieces were rehydrated in 20 μl of 40 mM ABC, 10% ACN, pH 8.0, containing 12.5 μg/ml sequencing grade modified trypsin (Promega). Proteins were digested overnight at 37 °C. After digestion, the gel pieces were shrunk with 100% ACN, and peptides were extracted with 0.2% TFA. Peptides were then desalted using C_{18} phase on a ZipPlate. Two elutions were performed successively to recover products from the C_{18} phase, first with 50% ACN, 0.1% TFA and then using 90% ACN, 0.1% TFA. Pooled elutions were concentrated using a vacuum centrifuge (Ep-

pendorf), and generated peptides were redissolved in 3 μl of 1% formic acid before mass spectrometry analysis.

Protein Identification by MALDI-TOF Mass Spectrometry—Digested samples were spotted directly onto a 96 × 2 MALDI plate (Applied Biosystems) using the dried droplet method (0.5 μl of the sample mixed on the plate with 0.5 μl of α-cyano-4-hydroxycinnamic acid matrix in ACN/water/TFA (50:50:0.1%). Droplets were allowed to dry at room temperature. Mass spectrometry analysis were performed on a MALDI-TOF Voyager DE-PRO mass spectrometer (Applied Biosystems) and acquired in positive ion reflector mode. Spectra were obtained in a reflectron-delayed extraction in source over a mass range of 500–3500 daltons. Raw spectra were treated automatically according to the Mascot wizard algorithm (version 1.1.2.0, Matrix Science) using the default parameters with the exception of the maximum peak count reduced to a value corresponding to the expected number of tryptic peptides according to the experimental molecular weight of the protein. The protein database was restricted to the rodent entries of the comprehensive nonredundant protein sequence database (NCBInr database; National Center for Biotechnology Information) (from version October 2005, 118,719 entries to version October 2007, 217,820 entries). When non-significant scoring was obtained, a manual treatment was performed according to the following explanations. First raw spectra were treated using a noise filter algorithm (correlation factor, 0.7) and the default advanced base-line correction. Then monoisotopic masses were generated on a fully detected spectrum after internal calibration using autodigestion tryptic peptides or external calibration using a mixture of five external standards (PepMix 1, LaserBio Labs, Sophia Antipolis, France). Mains peaks were selected according to local background, molecular weight of the protein, and known peak contamination from trypsin and keratin using PeakErazor software (version 1.49, Lighthouse Data, Odense, Denmark). Searches were carried out using four different algorithms for protein identification: Mascot (version 2.1, Matrix Science), ProFound (version 2005.02.14, Proteometrics), MS-Fit (version 3.2.1, ProteinProspector), and Aldente (version 2006.09.11, ExPASy) softwares on the rodent entries of the NCBInr database. A combination of results from different algorithms offers the option to cross-validate and consolidate the identification through the complementary use of several packages. Allowed variable modifications were oxidation of methionine, acrylamide-modified cysteine, and carbamidomethylation of cysteine. Up to one missed tryptic cleavage was considered, and a mass accuracy in the range of 25–50 ppm was used for all tryptic mass searches. Identification was considered positive if the protein was identified with the most elevated score using at least two algorithms. For a protein with a score close to the threshold value, the identification was rejected. Identified proteins are listed in Tables I and II. If peptides matched to multiple members of a protein family, the protein with the highest number of matched peptides and experimental molecular weight and isoelectric point close to theoretical parameters was indicated in the table, and NCBI accession numbers of the other isoforms are mentioned at the bottom of the table.

Antibodies—Monoclonal anti-14-3-3 β and anti-PP2A (catalytic subunit, clone 1D6) and polyclonal anti-$G_{i3}\alpha$, anti-neuronal NO synthase (nNOS), anti-panPKCs, anti-PKC ζ, anti-14-3-3 ζ, anti-PP2A-A α/β (regulatory subunit), and anti-c-Myc antibodies were purchased from Santa Cruz Biotechnology. Monoclonal anti-postsynaptic density (PSD)-95 antibodies (clone K28/86.2) were from Upstate Biotechnology. Polyclonal anti-FLAG and monoclonal anti-tubulin α (clone DM 1A), anti-tubulin β (clone TUB 2.1), anti-tubulin γ (clone GTU-88), and anti-FLAG M2 antibodies were from Sigma. Monoclonal anti-HA (clone 12CA5) and anti-G protein-coupled receptor kinase (GRK) 2/3 (clone C5/1.1) antibodies were purchased from Roche Diagnostics and Millipore, respectively. Cy™3-conjugated goat anti-mouse antibodies were from Jackson ImmunoResearch Laboratories, and horseradish peroxidase-conjugated secondary antibody was from Pierce. Polyclonal anti-otubain 1 and anti-MUPP1 antibodies were a kind gift from Dr. M. Y. Balakirev (Grenoble, France) and Dr. R. T. Javier (Houston, TX), respectively. Polyclonal anti-RGSZ1 antibodies were kindly provided by Dr. J. Garzon (Madrid, Spain).

Plasmids—The cDNA encoding HA-RGSZ1 was purchased from the University of Missouri Rolla cDNA Resource Center (Rolla, MO), and pGEX-4T-1 vector was from Amersham Biosciences. The cDNA encoding Myc-RGS10 was a kind gift from Dr. P. J. Casey (Durham, NC). The FLAG-MT_1 protein construct has been described elsewhere (16). The FLAG-MT_2 construct was obtained by a PCR-based approach using a Myc-MT_2 cDNA (16) and the Phusion High-Fidelity DNA Polymerase (Finnzymes). Restriction sites for EcoRI and XbaI were introduced immediately adjacent to the initiation and termination codons of MT_2 by PCR. After digestion by the respective restriction enzymes, the resulting insert was ligated into a pcDNA3.1 vector encoding FLAG. All constructs were confirmed by sequencing.

Cell Culture and Transfection—HEK 293 cells were grown in Dulbecco's modified Eagle's medium supplemented with 10% fetal calf serum, 100 units/ml penicillin, 0.1 mg/ml streptomycin, 0.02 M HEPES and transfected at 40–50% confluence using FuGENE 6 (Roche Applied Science).

Immunoprecipitation—HEK 293 cells grown in 100-mm culture dishes were transiently transfected by 4 μg of either FLAG-MT_1 or FLAG-MT_2 cDNAs together with 4 μg of HA-RGSZ1 or Myc-RGS10 cDNAs. 48 post-transfection, cells were stimulated, or not, by 10^{-7} M melatonin for 15 min at 37 °C, washed three times in PBS, and lysed in 1.5 ml of cold lysis buffer (75 mM Tris, 2 mM EDTA, 12 mM $MgCl_2$, 10 mM CHAPS, pH 7.4). After sonication, receptors were solubilized for 3 h at 4 °C under gentle end-over-end mixing, and lysates were centrifuged at 12,000 × *g* for 1 h at 4 °C. Receptor immunoprecipitation was performed on 1 ml of supernatant using 4 μg of polyclonal anti-FLAG antibodies preadsorbed on protein G-Sepharose beads (Sigma). Immunoprecipitated proteins were eluted with 50 μl of SDS-PAGE sample buffer (62.5 mM Tris/HCl, pH 6.8, 2% SDS, 10% glycerol, 100 mM DTT, 0.5% bromphenol blue) for 10 min at 95 °C and subjected to SDS-PAGE and immunoblotting.

Immunoblotting—Proteins resolved by 1D electrophoresis were transferred onto nitrocellulose membrane (Whatman GmbH). After incubation in PBS supplemented with 5% skimmed milk and 0.05% Tween 20 for 1 h at room temperature, membranes were incubated in primary antibody solution in PBS supplemented with 5% skimmed milk and 0.05% Tween 20 for an additional 1 h at room temperature. After washes in PBS supplemented with 0.05% Tween 20, immunoreactivity was revealed using a horseradish peroxidase-conjugated secondary antibody (1:10,000) and the ECL chemiluminescent reagent (Perbio).

Immunofluorescence Microscopy—HEK 293 cells transiently transfected by 2 μg of FLAG-MT_1 together with 1 μg of RGSZ1-YFP cDNA were grown on sterile coverslips. 48 post-transfection, cells were stimulated, or not, by 10^{-7} M melatonin for 15 min at 37 °C, washed three times in PBS, and fixed with 4% paraformaldehyde in PBS for 15 min. After blocking with 3% BSA in PBS for 30 min, cells were incubated with monoclonal anti-FLAG M2 (1:500) antibodies in PBS containing 0.3% BSA for 1 h at room temperature. Coverslips were then washed three times with PBS and incubated with Cy3-conjugated goat anti-mouse antibodies (1:800) in PBS containing 0.3% BSA for 40 min at room temperature. Coverslips were mounted and analyzed by confocal laser microscopy (Leica TCS SP2 AOBS).

Production and Purification of HA-RGSZ1—To express HA-RGSZ1 as a GST fusion protein, restriction sites for BamHI and XhoI were introduced immediately adjacent to the initiation and termination codons by PCR of the plasmid encoding HA-RGSZ1 using the Phu-

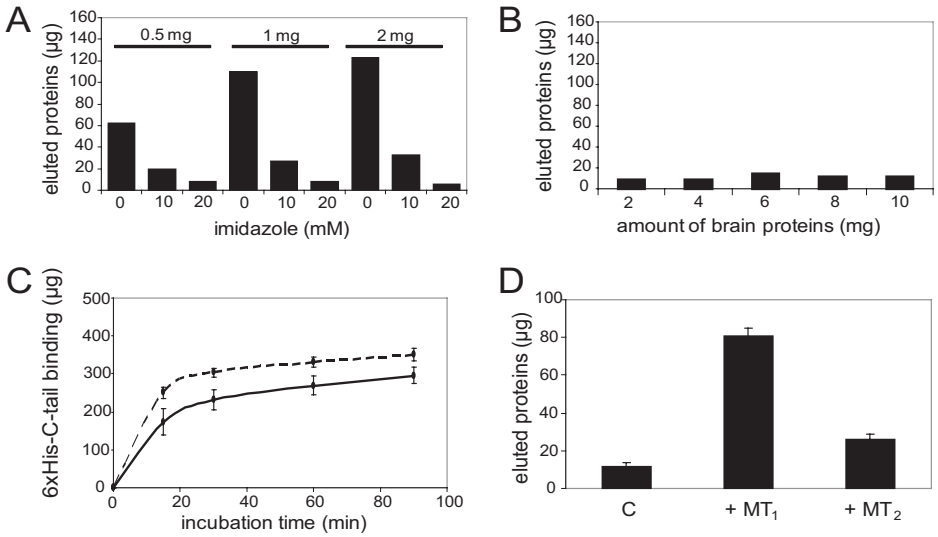

FIG. 1. **Optimization of the peptide affinity chromatography conditions.** *A*, determination of the optimal concentration of imidazole to minimize nonspecific binding on the beads. Different amounts of brain proteins were added to non-coated beads (20 μl) and incubated overnight at 4 °C in the presence or absence of 10 or 20 mM imidazole. After washes, proteins were eluted from the beads, and the nonspecific binding was quantified. *B*, determination of the optimal amount of brain protein lysates. Non-coated beads (20 μl) were incubated with 2, 4, 6, 8, or 10 mg of protein lysates in the presence of 20 mM imidazole overnight at 4 °C. After washes, proteins were eluted from the beads, and the nonspecific binding was quantified. *C*, determination of the binding kinetics of the His_6 (*6xHis*)-tagged peptides to the beads. 500 μg of His_6-tagged peptides were dissolved in a binding buffer containing 20 mM NaH_2PO_4, 6 M urea, pH 8, at 1 mg/ml. Absorbance of the peptide solutions was measured at 280 nm after 15, 30, 60, and 90 min of incubation with beads. *D*, determination of the amount of brain proteins specifically recruited by the C-tails of MT_1 and MT_2. 10 mg of brain protein lysate were incubated with 20 μl of beads coated with His_6-tagged baits in the presence of 20 mM imidazole overnight at 4 °C. After washes, the amount of retained proteins was quantified. *C*, non-coated beads. Results are expressed as mean ± S.E. ($n = 5$ for non-coated beads, $n = 3$ for MT_1, and $n = 6$ for MT_2).

sion High-Fidelity DNA Polymerase. After digestion by BamHI and XhoI, the resulting insert was ligated into pGEX-4T-1 vector. DNA sequences were confirmed by sequencing. The resulting plasmid was transformed into BL21(DE3) cells (Invitrogen), and cells were grown in LB medium containing 50 μg/ml ampicillin. Expression of GST-HA-RGSZ1 protein was induced by adding 1 mM isopropylthiogalactoside (Sigma) to midlog cultures. Cultures were harvested after 7 h at 37 °C. Cells were centrifuged at 6000 × *g* for 15 min, and the pellet was stored at −20 °C. For purification of HA-RGSZ1, the pellet was resuspended in cold PBS containing protease inhibitor mixture EDTA-free, crushed with an Ultra-Turrax T25, and sonicated. After adding 1% Triton X-100 (Sigma), the cell suspension was centrifuged at 10,000 × *g* for 30 min, and the supernatant was collected and applied to glutathione-agarose beads (Sigma) that had been equilibrated with 1% Triton X-100 in PBS. After extensive washes, HA-RGSZ1 proteins were eluted by 0.04 unit/μl thrombin (Amersham Biosciences) in 200 μl of PBS (2 h at 22 °C). Eluates were applied to new, freshly prepared glutathione-agarose beads to eliminate residual contaminant GST and bacterial proteins. The purity of HA-RGSZ1 was assessed by SDS-PAGE after silver staining.

[^{35}S]GTPγS Binding—[^{35}S]GTPγS binding was determined in 100 μl of reaction mixture containing 20 mM HEPES, 100 mM NaCl, 20 μg/ml saponin, 3 μM GDP, 3 mM $MgCl_2$, protease inhibitor mixture EDTA-free, pH 7.4. The reaction mixture also contained CHO cell membranes stably expressing the MT_1 receptor (5 fmol), 0.2 nM [^{35}S]GTPγS, and purified RGSZ1 with or without 1 μM melatonin. The reaction was started at 37 °C by adding [^{35}S]GTPγS and stopped at 60 min by filtration. Filters were washed with 50 mM Tris/HCl, pH 7.4, and radioactivity was measured.

Radioligand Binding—Ovine pituitary pars tuberalis was collected, and crude membranes were prepared essentially as described previously (17). Radioligand binding was performed with pars tuberalis membranes (1.5–2 mg of protein) in 1 ml of TEM buffer (75 mM Tris, 12 mM $MgCl_2$, 2 mM EDTA, protease inhibitor mixture EDTA-free, pH 7.4) containing 400 pM 2-[^{125}I]melatonin (PerkinElmer Life Sciences) for 90 min at 37 °C. After membrane solubilization with 1% digitonin (overnight at 4 °C) and centrifugation (90 min at 18,000 × *g* at 4 °C), RGSZ1 was immunoprecipitated from solubilized proteins using 10 μl of polyclonal anti-RGSZ1 antibodies preadsorbed on protein G-Sepharose beads. Beads were washed, and radioactivity was measured after rapid filtration through GF/F glass fiber filters (Whatman).

RESULTS

Optimization of the Peptide Affinity Chromatography—Metal affinity chromatography on an Ni-NTA matrix was chosen to purify proteins interacting with the amino-terminally His_6-tagged C-tails of MT_1 and MT_2 (61 and 59 amino acids long, respectively) in whole brain lysates. Binding of His_6-tagged proteins is maintained under low concentrations of imidazole, which is known to minimize nonspecific binding to Ni-NTA-agarose beads by competing for nickel ion binding with dispersed histidine residues in proteins. To determine the optimal imidazole concentration, beads were incubated with different amounts of brain lysates in the presence of different imidazole concentrations. After several washes, retained proteins were recovered and quantified (Fig. 1*A*). In the absence of imidazole, the nonspecific binding was high and increased concurrently to the amount of brain proteins added. At 20 mM, the nonspecific binding was dramatically decreased irrespective of the amount of lysate used. Further increase in the

amount of brain lysate (up to 10 mg of protein) did not change the level of nonspecific binding (10–12 μg) (Fig. 1*B*). We thus incubated Ni-NTA beads with 10 mg of brain lysate in the presence of 20 mM imidazole in all further experiments.

We then determined the binding kinetics of the His_6-tagged peptides to the Ni-NTA beads in phosphate buffer at pH 8, the optimal pH for binding of His_6-tagged peptides (according to the manufacturer) and for the preservation of protein complexes (18). Binding of peptides was rapid and reached a plateau after 30 min. After 90 min, 295 ± 21 μg ($n = 4$) and 351 ± 16 μg ($n = 4$) of His_6 MT_1 and MT_2 C-tails, respectively, were immobilized on Ni-NTA beads (Fig. 1*C*). Using these optimized experimental settings, the C-tails of MT_1 and MT_2 typically recruited 80.7 ± 4.3 μg ($n = 3$) and 26.4 ± 2.7 μg ($n = 6$) of proteins, respectively. Under our conditions, nonspecific binding in the absence of peptide was 11.9 ± 1.4 μg ($n = 6$).

Functional Validation of Peptide Columns—We used the differential presence of a PSD-95/Disc-large/ZO-1 (PDZ) domain binding motif in the C-tails of MT_1 and MT_2 to evaluate the efficacy and specificity of our purification approach. Whereas the C-tail of MT_1 contains a functional class III PDZ recognition motif, MT_2 does not. PDZ domain-containing proteins are prototypical scaffolding proteins that are involved in the assembly of large molecular complexes. Based on literature reports (19, 20) and our own results[2] obtained from a yeast two-hybrid screen, we probed eluates of the peptide columns for the presence of three PDZ domain-containing proteins, the multi-PDZ domain-containing protein MUPP1, nNOS, and PSD-95. The use of specific antibodies revealed the presence of MUPP1, nNOS, and PSD-95 in eluates of the MT_1 C-tail column but not in that of control or MT_2 C-tail columns (Fig. 2). These results confirm the high specificity of our approach. In addition, we identified three PDZ domain-containing proteins as new interacting proteins for MT_1. We furthermore probed the column eluates for the presence of GRKs, which are known as specific GPCR-associated proteins (21). Indeed GRK2/3-specific antibodies confirmed the presence of these kinases in eluates of MT_1 and MT_2 C-tail columns (Fig. 2). We finally probed eluates of the peptide columns for the presence of the α subunit of the heterotrimeric G_i proteins known to be associated with the MT_1 and MT_2 receptors (22–24). As shown in Fig. 2, the MT_1 C-tail and, to a lesser extent, the MT_2 C-tail retained $G_{i3}\alpha$ proteins.

Systematic Identification of MT_1- and MT_2-associated Proteins—We then performed large scale experiments to recover protein quantities that are sufficient for mass spectrometric analysis. Because of the inherent limitations of the different electrophoretic approaches, peptide column eluates were separated in three different ways: 2D electrophoresis (150–180 μg of recruited proteins) and 1D electrophoresis using either 10 or 5–9% polyacrylamide gradient gels. Fig. 3 illustrates a typical gel for each condition. Numerous 2D spots

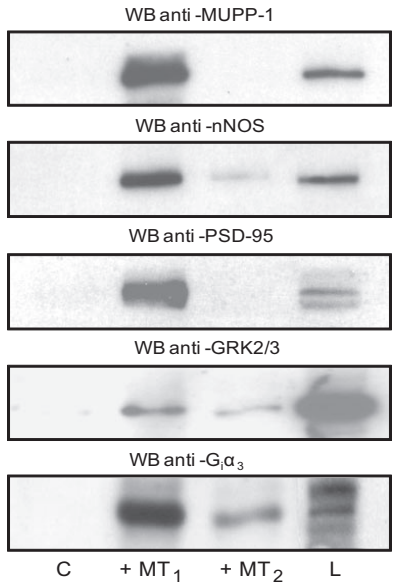

FIG. 2. **Detection of PDZ domain-containing proteins, $G_{i3}\alpha$, and GRK2/3 by immunoblotting.** 20 μl of beads coated with His_6-tagged MT_1 and MT_2 C-tails were incubated with 10 mg of protein lysates from mouse brain. Beads were washed, and recruited proteins were eluted with 50 μl of 2% SDS in PBS. 10 μl were separated by SDS-PAGE and transferred to nitrocellulose membranes. Immunoblotting was performed with antibodies raised against three PDZ domain-containing proteins, polyclonal anti-MUPP1 (1:10,000), polyclonal anti-nNOS (1:1000) and monoclonal anti-PSD-95 (1:2000); against $G_{i3}\alpha$ (1:1000); and against GRK2/3 (1:1000). *C*, negative control, beads without peptide; *L*, brain lysate (20 μg). *WB*, Western blot.

and 1D bands were reproducibly observed on silver-stained gels for MT_1 and MT_2 conditions. In agreement with Fig. 1*A*, the apparent number of proteins recruited by the C-tail of MT_1 was greater than for MT_2. 1D and 2D control gels showed that non-coated beads recruited very few nonspecific proteins. Silver-stained 2D spots and 1D bands were systematically excised and digested with trypsin, and the resulting peptides were analyzed by MALDI-TOF and identified automatically with the Mascot wizard algorithm or manually with Mascot, ProFound, MS-Fit, and Aldente softwares in the NCBInr database. Proteins unambiguously identified by mass spectrometry for the C-tails of MT_1 and MT_2 and for the non-coated beads are listed in Tables I and II and supplemental Table 1, respectively. We identified 58 proteins that were retained by the non-coated beads. These proteins, having affinity for Ni-NTA-agarose beads, were considered as nonspecific binders and systematically removed when found in the lists of MT_1- and MT_2-interacting proteins. 40 proteins that bind to the C-tail of MT_1 and 22 proteins that bind to the C-tail of MT_2 were identified. Among the 40 proteins identified for the MT_1 C-tail, 30 were obtained from 2D electrophoresis, and 10 were obtained from 1D electrophoresis. Among the 22 proteins identified for the MT_2 C-tail, 11 were obtained from 2D electrophoresis, and 11 were obtained from 1D electrophoresis. For each C-tail, different α and β isoforms of tubulin were

[2] J. Guillaume and R. Jockers, unpublished data.

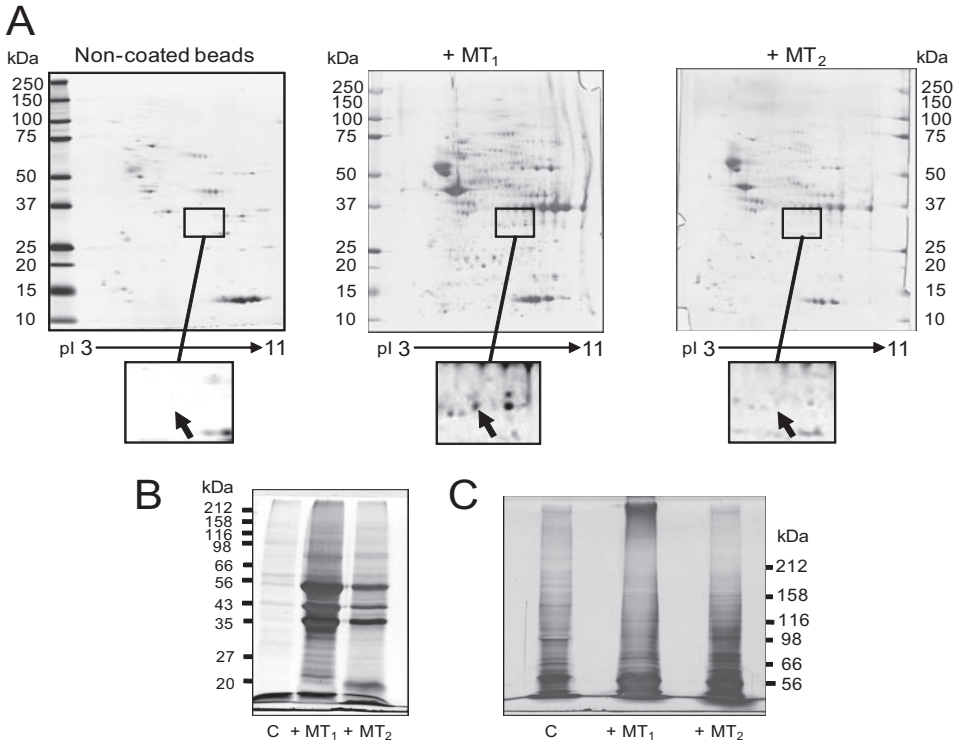

FIG. 3. **2D and 1D electrophoresis separation of the MT_1 and MT_2 C-tail-associated protein complexes.** Mouse brain protein complexes recruited by the Ni-NTA-immobilized C-tail of MT_1 and MT_2 receptors were separated by 2D (*A*) or 1D electrophoresis on a 10% (*B*) or 5–9% gradient polyacrylamide gel (*C*) and silver-stained. A typical gel for each condition is shown. *C*, negative control, beads without peptide. The *arrows* indicate the position of RGSZ1.

identified from 1D electrophoresis (10 and 5–9% gradient gels), but the corresponding spots, although easily noticeable from 2D gels, were not excised for identification. If α and β isoforms of tubulin are not taken into account, separation of samples by 1D electrophoresis allowed the identification of eight and nine additional high molecular mass proteins (including seven proteins of molecular mass $\geq$150 kDa) for MT_1 and MT_2, respectively. This significant increase in the number of identified interacting proteins (20% of the MT_1 and 41% of the MT_2 interactomes) clearly illustrates that separation of column eluates by 1D electrophoresis is complementary to 2D electrophoresis. Identified proteins showed localization to different subcellular compartments (plasma membrane, cytosol, and cytoskeleton) and could be divided into five distinct groups: "membrane proteins," "signaling proteins," "cytoskeleton proteins," "chaperones and stress response proteins," and a last group, classified as "others," containing the remaining proteins for which the function is not well described.

Validation of MT_1- and MT_2-associated Proteins by Immunoblotting Screen—Using specific antibodies, we next performed an immunoblotting screen to estimate the overall reliability of our mass spectrometry data and to quantify the relative amount of proteins that are recruited by both C-tails. Seven different antibodies were tested and confirmed the presence of the interacting protein identified by MALDI-TOF, demonstrating the high quality of our mass spectrometric data (Fig. 4). These experiments validated common interaction partners for both receptors, such as the tubulin α and β isoforms, the catalytic subunit of the protein phosphatase PP2A, and the PKC ζ2, and showed higher recruitment with the C-tail of MT_1 compared with MT_2. The immunoblotting screen also confirmed MT_1-specific interacting partners, such as 14-3-3 β; the ubiquitin thiolesterase otubain 1 (OTUB1), which is known to express different alternatively spliced forms (25); and an RGSZ1 splice variant migrating at 36 kDa as reported previously in bovine brain (26). In addition, validation of 14-3-3 β, otubain 1, and the catalytic subunit of PP2A demonstrates the reliability of MALDI-TOF identifications from 1D gels. Using other antibodies, we also demonstrated the presence of the regulatory subunit Aα/β associated with the catalytic subunit of PP2A and another isoform of 14-3-3 (14-3-3 ζ) in the MT_1 C-tail eluates (supplemental Fig. 1). Both C-tails also recruited the γ isoform of tubulin.

Validation of the Interaction between the MT_1 Receptor and RGSZ1 in Living Cells—RGS proteins are signaling modulators of heterotrimeric Gα proteins that increase their rate of GTP hydrolysis. Recent observations indicate that RGS proteins regulate G protein-dependent signaling not only in a G protein-specific manner but also in a receptor-specific manner (27–30). The molecular basis for receptor specificity is still poorly understood. However, the recruitment of RGS proteins into receptor-associated complexes, as suggested by our

TABLE I

MALDI-TOF mass spectrometry identification of protein complexes associated with the C-tail of MT_1 receptor

Trypsin-digested proteins were analyzed by MALDI-TOF, and searches were carried out automatically using Mascot wizard software or manually using four different algorithms (Mascot, ProFound, MS-Fit, and Aldente) from the comprehensive nonredundant protein sequence database NCBInr. ND, not determined; CLIP, cytoplasmic linker protein.

NCBI accession no.	Protein identity	Theoretical parameters		Observed parameters		Matched peaks/ selected peaks	Sequence coverage	Electrophoretic separation	Identified with MT_2
		Molecular mass	pI	Molecular mass	pI				
		kDa		*kDa*			%		
Membrane protein									
47059002	Solute carrier family 4, sodium bicarbonate cotransporter, member 5	124	8.4	125	6.5	9/46	13	2D	–
109459952	Similar to transient receptor potential cation channel, subfamily M, member 6	248	8.7	158	ND	16/58	10	1D (5–9%)	–
17481296	Vomeronasal receptor 1 A12	35	9.3	28	7.8	5/35	25	2D	–
Signal transduction									
3065925	14-3-3 protein β	28	4.8	31	ND	7/39	36	1D	–
15928666	Adenylate kinase isoenzyme 1	22	5.7	21	4.5	6/25	34	2D	–
3024067	Casein kinase II subunit α	45	7.9	43	7.5	5/26	25	2D	+
6753490	COP9 signalosome subunit 4	47	5.6	42	5.8	9/54	37	2D	–
21312314	Dual specificity protein phosphatase 3	20	6.6	20	6.1	10/38	61	2D	+
81912670	PKC ζ2	47	4.7	60	7.5	5/22	26	2D	+
17512397	Ppp2cb protein	32	5.5	32	ND	7/44	28	1D	–
41152502	Rabphilin 3A-like (Noc2)	34	9.1	26	7.7	9/53	25	2D	–
6180019	Regulator of G-protein signaling 20 (RGSZ1)	27	5.2	31	6.5	5/44	48	2D	–
45219891	Ubiquitin-specific peptidase 5 (isopeptidase T)	97	4.9	125	ND	12/62	16	1D (5–9%)	–
32484336	Ubiquitin thiolesterase (Otub1 protein)	31	4.8	32	ND	5/22	28	1D	–
Cytoskeleton									
22122615	ARP1 actin-related protein 1 homolog B	42	6.0	45	6.8	7/47	30	2D	–
13508541	CLIP-associating protein 1	44	6.6	44	8.6	13/68	56	2D	–
6680924	Cofilin-1 (nonmuscle isoform)	19	8.2	18	9.1	9/45	57	2D	–
6671746	Cofilin-2 (muscle isoform)	19	7.6	18	8.2	7/38	48	2D	–
24657655	Cytoplasmic linker protein 2	112	6.1	88	9.0	8/53	18	2D	–
9790219	Destrin	19	8.2	17	9.1	11/26	50	2D	–
487851	Dynamin	85	6.0	105	7.8	13.36	20	2D	–
35193307	Dynamin 1	96	6.6	105	7.6	9/43	8	2D	–
14193692	Glial fibrillary acidic protein	47	5.0	43	7.5	5/25	16	2D	–
25955543	Glial maturation factor, β	17	5.1	17	5.3	4/25	38	2D	+
2119280	Kinesin	101	5.6	158	ND	11/58	15	1D (5–9%)	–
18859641	Myosin heavy polypeptide 7	222	5.6	100	ND	23/76	16	1D (5–9%)	–
62825944	Tubulin, α1C[a]	50	4.9	160	ND	13/73	46	1D/1D (5–9%)	+
21595026	Tubulin, β3[b]	50	4.8	50	ND	7/34	24	1D/1D (5–9%)	+
Chaperone and stress response									
6671702	Chaperonin subunit 5 (ϵ)	60	6.0	65	6.2	9/42	38	2D	–
126521835	Chaperonin subunit 2 (β)	58	6.0	56	6.7	17/78	43	2D	–
110625998	DnaJ homolog, subfamily B, member 11	41	5.9	40	7.1	9/36	37	2D	–
Others									
40068507	Collapsin response mediator protein (CRMP) 1	62	6.6	64	7.4	8/44	21	2D	–
24418919	Brain glycogen phosphorylase	96	6.3	105	ND	22/82	33	1D (5–9%)	+
40254595	Dihydropyrimidinase-like 2	63	6.0	66	6.9	21/47	61	2D	+
21362303	Hypothetical protein LOC-67826	47	5.5	47	6.1	14/50	48	2D	–
21313286	Hypothetical protein LOC-76824	32	5.8	40	6.3	5/26	22	2D	–
12857982	Unnamed protein product	18	6.1	18	6.1	7/27	62	2D	–
12860873	Unnamed protein product	29	5.4	25	5.2	4/28	14	2D	–
26344447	Unnamed protein product	40	6.2	48	5.8	9/52	30	2D	–
7422551	Unnamed protein product	72	5.0	72	5.4	15/77	32	2D	–

[a] Other isoforms of tubulin α chain were identified (NCBI accession numbers 32015, 202225, 6678469, 6755901, 27762594, 34740335, 54035478, and 80474380).

[b] Other isoforms of tubulin β were identified (NCBI accession numbers 29145006 and 31981939).

TABLE II

MALDI-TOF mass spectrometry identification of protein complexes associated with the C-tail of MT_2 receptor

Trypsin-digested proteins were analyzed by MALDI-TOF, and searches were carried out automatically using Mascot wizard software or manually using four different algorithms (Mascot, ProFound, MS-Fit, and Aldente) from the comprehensive nonredundant protein sequence database NCBInr. ND, not determined.

NCBI accession no.	Protein identity	Protein parameters		Observed parameters		Matched peaks/ selected peaks	Sequence coverage	Electrophoretic separation	Identified with MT_1
		Molecular mass	pI	Molecular mass	pI				
		kDa		*kDa*			%		
Membrane protein									
6978547	Na^+/K^+-ATPase α3 subunit	113	5.3	105	ND	12/59	16	1D (5–9%)	–
26251984	Na^+/K^+-ATPase 3 (fragment)	33	5.2	33	8.5	4/27	30	2D	–
62660468	Similar to WD repeat membrane protein	150	5.9	125	ND	12/66	10	1D (5–9%)	–
Signal transduction									
1262300	Casein kinase II α subunit	45	7.9	38	9.5	5/46	23	2D	+
400704	Catenin δ-1 (p120-catenin)	102	6.5	110	ND	10/55	16	1D (5–9%)	–
56205529	Clathrin heavy polypeptide	194	5.5	180	ND	16/39	13	1D (5–9%)	–
21312314	Dual specificity phosphatase 3	21	6.1	21	6.1	7/58	50	2D	+
33438248	MKIAA0034 protein (clathrin heavy chain)	192	5.4	190	ND	22/67	17	1D (5–9%)	–
31158356	PKC ζ2	47	4.7	41	9.0	6/44	28	2D	+
45477181	Tyrosine-protein phosphatase, nonreceptor type 13	272	5.9	250	ND	7/20	5	1D (5–9%)	–
Cytoskeleton									
11993948	Glial maturation factor β	17	5.3	18	4.6	5/24	38	2D	+
547890	Microtubule-associated protein 2	203	4.8	250	ND	8/34	7	1D (5–9%)	–
6678469	Tubulin, α1C[a]	50	4.9	55	ND	9/49	30	1D/1D (5–9%)	+
12963615	Tubulin β3[b]	50	4.8	60	ND	13/46	44	1D/1D (5–9%)	+
Chaperone and stress response									
6754256	Heat shock protein 9	74	5.9	75	5.9	12/61	23	2D	–
97536358	Heat shock protein, 105 kDa (HSP-E7I)	96	5.4	65	4.5	6/41	13	2D	–
Others									
24418919	Brain glycogen phosphorylase	97	6.3	100	ND	14/51	21	1D (5–9%)	+
7710012	Crystallin, μ	34	5.4	35	5.3	4/40	23	2D	–
40254595	Dihydropyrimidinase-like 2	63	6.0	70	7.0	13/64	31	2D	+
66912155	mUp76 (Calpain 3)	77	5.6	60	7.7	8/38	25	2D	–
1334146	Unnamed protein product	30	5.3	29	4.2	5/36	32	2D	–
26326811	Unnamed protein product	120	8.8	158	ND	10/66	16	1D (5–9%)	–

[a] Other isoform of tubulin α chain was identified (NCBI accession number 32015).

[b] Other isoforms of tubulin β chain were identified (NCBI accession numbers 13542680 and 62663465).

data, represents one possible explanation. To confirm the physiological association of RGSZ1 with the full-length MT_1 receptor, we co-expressed either FLAG-MT_1 or FLAG-MT_2 constructs together with HA-tagged RGSZ1 in HEK 293 cells. Co-immunoprecipitation experiments performed with anti-FLAG antibodies revealed that only MT_1 co-immunoprecipitated RGSZ1 in both resting and melatonin-activated cells (Fig. 5*A*). The specificity of the interaction was further validated using RGS10 as a negative control. As shown in Fig. 5*B*, immunoprecipitation of FLAG-MT_1 or FLAG-MT_2 did not co-immunoprecipitate RGS10. As an additional control, we further performed immunofluorescence experiments in HEK 293 cells co-expressing FLAG-MT_1 together with RGSZ1-YFP (Fig. 5*C*). Consistent with our biochemical experiments, a distinct co-localization at the plasma membrane was observed in these cells irrespective of the activation state of the receptor.

To evaluate the functional relevance of RGSZ1 coupling to the MT_1 receptor, we determined the effect of increasing concentrations of purified RGSZ1 on [^{35}S]GTPγS binding in response to 1 μM melatonin using CHO cell membranes stably expressing high levels of MT_1 (Fig. 5*D*). As expected, the agonist melatonin stimulated [^{35}S]GTPγS binding (to 221 $\pm$ 27%), indicating efficient MT_1 protein coupling in the absence of RGSZ1. When purified RGSZ1 was added, an increase in the [^{35}S]GTPγS binding was observed in response to the agonist as reported previously for RGS4 (31). This assay is designed to promote [^{35}S]GTPγS binding in the presence of RGS proteins as GTP hydrolysis becomes rate-limiting due to saturation of GDP-GTP exchange at high concentrations of receptor (31). This results in local depletion of inactive heterotrimeric G-GDP that is reversed by RGS GTPase-activating protein activity. Indeed purified RGSZ1 accelerated melatonin-promoted [^{35}S]GTPγS bind-

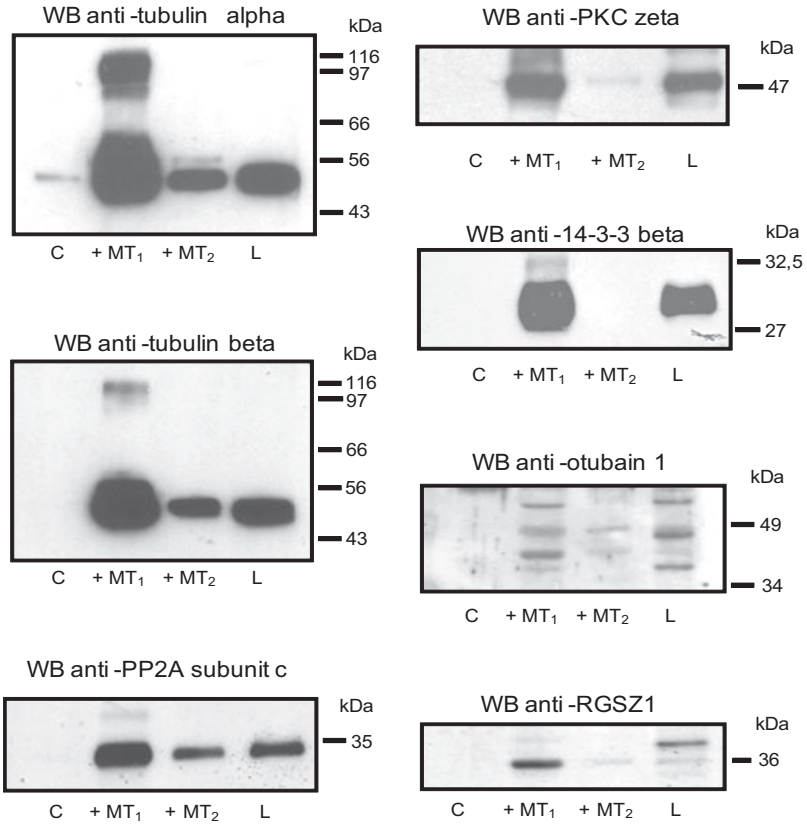

FIG. 4. **Validation of MALDI-TOF-identified binding proteins by immunoblotting.** Immobilized His_6-tagged MT_1 and MT_2 C-tails were incubated with 10 mg of protein lysates from mouse brain. Recruited proteins were eluted with 50 μl of 2% SDS in PBS. 10 μl were separated by SDS-PAGE and transferred to nitrocellulose membranes. Immunoblotting was performed with monoclonal anti-tubulin α (1:2000), monoclonal anti-tubulin β (1:2000), monoclonal anti-PP2A catalytic subunit (1:1000), polyclonal anti-PKC ζ (1:1000), monoclonal anti-14-3-3 β (1:1000), polyclonal anti-otubain 1 (1:2000), and polyclonal anti-murine RGSZ1 (1:500) antibodies. *C*, negative control, non-coated beads; *L*, brain lysate (20 μg). *WB*, Western blot.

ing, reaching maximal values at 10^{-8} M RGSZ1 (305 $\pm$ 8%, $p = 0.02$).

To confirm that the presence of RGSZ1 in MT_1-associated protein complexes is physiologically relevant, we performed immunoprecipitation studies with ovine pituitary pars tuberalis tissue samples known to express significant amounts of endogenous MT_1 receptors (32, 33) and RGSZ1 (data not shown). In the absence of high affinity anti-MT_1 antibodies, receptors were labeled with the specific 2-[^{125}I]iodomelatonin radioligand, and protein complexes were solubilized and immunoprecipitated with anti-RGSZ1 antibodies. As shown in Fig. 5*E*, significant amounts of radiolabeled MT_1 were precipitated in the presence of anti-RGSZ1 antibodies, demonstrating the existence of MT_1-RGSZ1 complexes in native tissue.

DISCUSSION

In this study, we present an improved proteomics approach coupling peptide affinity chromatography with 1D and 2D electrophoresis separation and mass spectrometry for the identification of proteins interacting with the C-tail of GPCRs. To date, this is the first study proposing the use of an adapted and optimized IMAC for the identification of protein complexes. Using this approach, we identified 40 proteins that bind to the C-tail of MT_1 and 22 proteins that bind to the C-tail of MT_2.

Interactions between GPCRs and associated proteins are known to involve the intracellular loops, the transmembrane, and the C-tail of GPCRs. The most abundant and the best studied are proteins interacting with the C-tail of GPCRs. This C-tail, recently nicknamed the "magic" tail by Bockaert *et al.* (7), serves as a scaffold for the formation of a signalosome containing diverse effectors and clustering proteins. The nature of the interaction proteins that bind to the C-tail of GPCRs can determine not only its targeting to a specific cellular compartment but also its association with other signaling or structural proteins and the fine tuning of its signal transduction such as desensitization and resensitization (34). Therefore, the identification of the protein complexes associated with GPCRs constitutes an important step toward the development of new drugs. Indeed these compounds could be used to disrupt or strengthen specific interactions between GPCRs and their associated proteins. Different proteomics approaches coupling peptide affinity chromatography and mass spectrometry have been developed to identify proteins interacting with the C-tail of GPCRs and have proven their efficacy in identifying protein complexes associated with the C-tail of GPCRs (7, 35). However, these approaches, which used either short peptides encompassing a specific interaction motif such as the PDZ ligand of the 5-HT_{2A} and 5-HT_{2C} receptors (12, 13) or the entire C-tail expressed as a GST fusion protein such as for the 5-HT_{2C} receptor (11), have shown limitations. They were either too restrictive to some particular interaction proteins (PDZ domain-containing proteins) or used GST fusion proteins as "bait" leading to increased background.

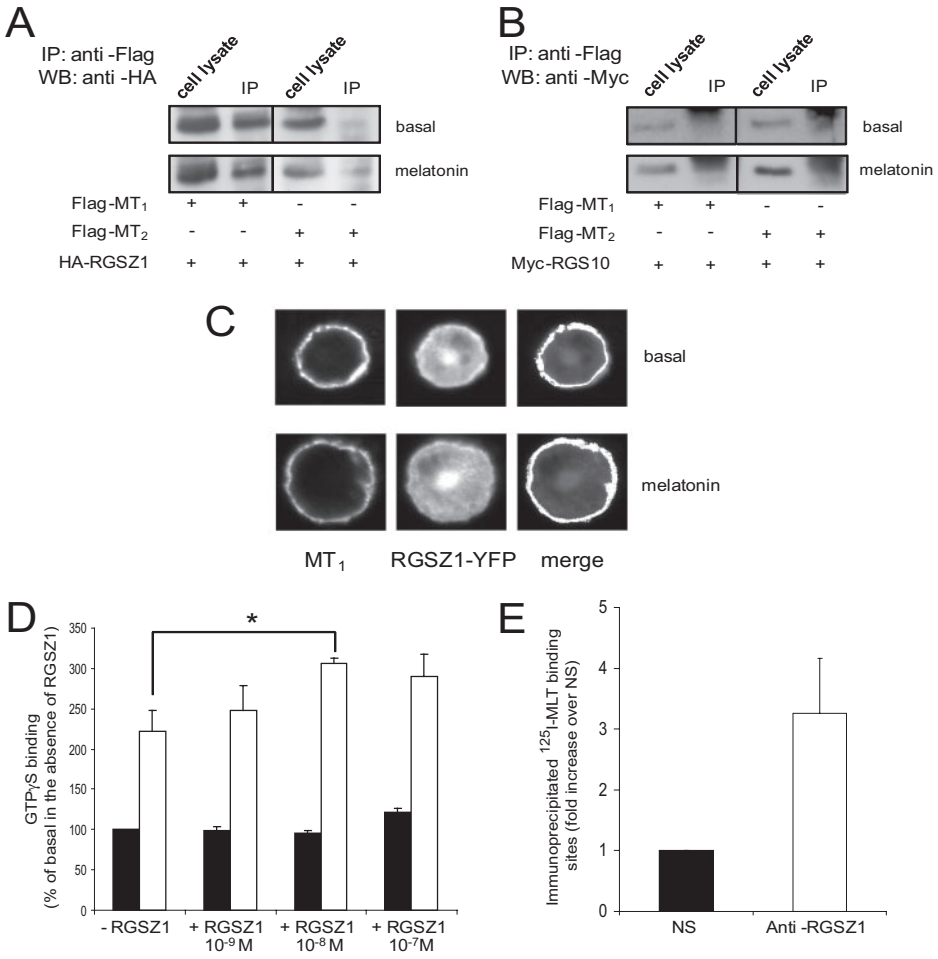

FIG. 5. **Functional interaction between RGSZ1 and MT_1 in cells.** HEK 293 cells transiently expressing either FLAG-MT_1 or FLAG-MT_2 were co-transfected with HA-RGSZ1 (*A*) or Myc-RGS10 (*B*). 48 h post-transfection, cells were stimulated, or not, by melatonin (10^{-7} M for 15 min) and lysed. The MT_1 and MT_2 receptors were immunoprecipitated by anti-FLAG antibodies, and precipitates were analyzed by Western blot for the presence of co-immunoprecipitated HA-RGSZ1 (*A*) or Myc-RGS10 (*B*) using anti-tag antibodies. *C*, confocal images of HEK 293 cells co-expressing FLAG-MT_1 with RGSZ1-YFP. Receptors were immunostained with anti-FLAG antibodies, and RGSZ1 was revealed by its YFP fluorescence. The co-localization of both proteins was evaluated with the ImageJ co-localization highlighter plug-in. *D*, [^{35}S]GTPγS binding to MT_1-expressing CHO cells without (*black bars*) or with 1 μM melatonin (*white bars*) in the absence or presence of the indicated concentrations of purified RGSZ1. Data represent the mean ± S.E. of three experiments, each conducted in triplicate. Statistical significance was determined using the Mann-Whitney test. *, $p < 0.05$. *E*, co-immunoprecipitation of ^{125}I-melatonin (*^{125}I-MLT*)-labeled MT_1 receptors with anti-RGSZ1 antibodies. Nonspecific binding was estimated by performing immunoprecipitation using a pool of five non-relevant polyclonal antibodies. Data represent the mean ± S.E. of two experiments. *IP*, immunoprecipitate; *WB*, Western blot; *NS*, nonspecific binding.

IMAC has several advantages. Indeed the Ni-NTA interaction with the His_6 tag is highly specific and strong enough to resist detergents, induces low nonspecific binding due to the addition of low concentrations of imidazole (Fig. 1*A*), and uses pH conditions optimal for the preservation of protein complexes and to minimize nonspecific interactions (18). Moreover the His_6 tag is much smaller (955 Da) than other commonly used tags, such as the GST tag (26 kDa), contributing to the reduction of nonspecific interactions between mice brain proteins and the tag. The use of chemically synthesized bait of high purity also considerably reduced nonspecific binding in contrast to GST-tagged bait produced in bacteria for which the 2D protein pattern is often complex due to the presence of bacterial proteins, which bind to the GST tag and/or fusion peptide during bait production in bacteria, and the major brain proteins. After optimizing parameters such as the concentration of imidazole, the amount of brain protein lysates, and the incubation time for bait coupling on the beads, we were able to considerably reduce nonspecific binding to 0.1% (10 μg from 10 mg of total brain proteins). Using these experimental settings, ~80 and 25 μg of brain proteins (from 10 mg) were specifically recruited by the C-tails of MT_1 and MT_2, respectively.

Most studies aiming to identify protein complexes associated to the C-tail of GPCRs have used 2D electrophoresis for protein separation. This technique minimizes the number of

potential candidates as it is not adapted for selection of hydrophobic, basic, and large proteins. To enlarge the number of interacting proteins and obtain a more detailed interactome, we performed 2D electrophoresis and 1D electrophoresis using 10 and 5–9% gradient gels. The utilization of 1D electrophoresis was possible because of the small size of the His_6-tagged baits (7.16 kDa for the MT_1 and 6.80 kDa for the MT_2 C-tails) in contrast to the larger GST baits whose size makes the use of 1D electrophoresis difficult notably for the identification of proteins with molecular weights similar to that of the bait. Among the 40 proteins identified for the MT_1 C-tail, 30 were obtained from 2D electrophoresis, and 10 were obtained from 1D electrophoresis. Among the 22 proteins identified for the MT_2 C-tail, 11 were obtained from 2D electrophoresis, and 11 were obtained from 1D electrophoresis. These results demonstrated that the combination of 1D and 2D electrophoresis greatly increased the number of proteins identified and that the use of only 2D electrophoresis led to an underestimation of multiprotein complexes associated to the C-tail of GPCRs. Identification of proteins by MALDI-TOF mass spectrometry, which only provides peptide mass fingerprints but no sequence information, is known to require prior high quality purification. However, our study has shown that several proteins separated by 1D electrophoresis could be unambiguously identified by MALDI-TOF because of the sensitivity of the apparatus and the stringency of our experimental conditions that considerably reduce the nonspecific binding and consequently the complexity of the protein electrophoretic pattern for MS identification.

Several previously described GPCR-associated proteins were identified. In this study, we showed that the C-tail of MT_1 recruited 14-3-3 β and destrin, proteins shown to be associated with mGluR5 (36), and dynamin 1, a protein known to interact with 5-HT_{2C} (11) and mGluR5 (36). Some proteins found in MT_2 C-tail eluates were also already described as GPCR-binding proteins, such as the clathrin heavy chain and Na^+/K^+-ATPase α3 subunit for mGluR5 (36) and microtubule-associated protein 2 (MAP2) for mGluR5 (36) and 5-HT4a (13). Ten common members of MT_1 and MT_2 C-tail-associated complexes were identified, including well known GPCR-associated proteins such as $G_i\alpha$ proteins and GRK2/3 and other proteins such as dual specificity phosphatase 3 (DSP3), a protein able to dephosphorylate protein substrates containing both phosphotyrosine and phosphoserine or phosphothreonine residues, with specificity for the mitogen-activated protein kinases (MAPKs) Erk2 and c-Jun NH_2-terminal kinase (JNK) (37). The serine/threonine protein kinase casein kinase II (CK2), recently shown to be involved in phosphorylation of the M3 muscarinic receptor (38), was also found as a common interaction member of MT_1 and MT_2 C-tails. Interestingly a role for CK2 consensus sites within GPCR C-tails has been proposed in targeting GPCRs to the β-arrestin-dependent pathway (39). PKC ζ2 and tubulins α and β were also recruited by both MT_1 and MT_2 C-tails and confirmed by immunoblotting. PKC ζ2 is specifically expressed in the mouse brain (40) and is a member of the atypical PKC subfamily. Tubulins α and β constitute the basic building block of microtubules, the major components of the cytoskeleton involved in many essential processes (41). Tubulins α and β have been shown to interact with the C-tails of mGluR7a and mGluR1a, respectively (42–44), and we recently demonstrated a modulation of melatonin receptors and G protein function by microtubules (45).

Among the proteins involved in signal transduction that were specifically recruited by the C-tail of MT_1, we identified two proteins involved in the deubiquitination pathway and members of the ubiquitin-specific processing proteases, otubain 1 (confirmed by Western blot) and ubiquitin-specific peptidase 5, also known as isopeptidase T. Subunit 4 of COP9, a multiprotein complex of the ubiquitin-proteasome pathway, was also identified. The β isoform of the catalytic subunit of protein phosphatase 2A (PPP2cb) was also found. PP2A is a highly conserved serine/threonine phosphatase that plays pivotal roles in diverse cellular functions (46). A direct interaction between this subunit and the C-tail of the ionotropic *N*-methyl-D-aspartate receptor has already been demonstrated by yeast two-hybrid and immunoprecipitation experiments (47). In addition, PP2A has been shown to co-immunoprecipitate with mGluR5 and regulates mGluR5-dependent mitogen-activated protein kinase/extracellular signal-regulated kinase kinase (MEK)/ERK phosphorylation in neurons (48). Finally three PDZ domain-containing proteins were also identified as specific MT_1-associated proteins by immunoblot: MUPP1, nNOS, and PSD-95. We failed to identify these three proteins by MS probably due to their low abundance within the gels. MUPP1 has been characterized previously as a direct interaction partner of MT_1 that promotes G_i protein coupling of this receptor (49). Neuronal NO synthase has been previously proposed as a potential interacting candidate of the MT_1 receptor (20). However, nothing is known about the functional consequences of this particular interaction. PSD-95 is a prototypical scaffolding protein highly enriched in the PSD that belongs to the membrane-associated guanylate kinase family (51). PSD-95 interacts with a host of proteins of diverse functions, most notably *N*-methyl-D-aspartate receptors, and regulates the functional integration of these receptors into signaling complexes in PSD (51). Interaction between PSD-95 and GPCRs has already been described as with the somatostatin receptors SSTR4 and SSTR1 (52) and dopamine D1 receptors (53). The coupling of PSD-95 with the C-tail of D1 receptors has been shown to regulate the surface expression and the intracellular trafficking of the receptors and to inhibit D1 receptor-mediated signaling in mammalian cells (53). $G_{i3}\alpha$ proteins were also detected by immunoblot but again failed to be identified by MS. In contrast, $G_i\alpha$ was easily detectable by MS using the tandem affinity purification (TAP) approach (24) suggesting that the C-tail of MT_1 and MT_2 is involved in $G_i\alpha$ binding but that

further molecular determinants provided by the entire receptor are needed for efficient $G_i\alpha$ recruitment.

By our approach, we were also able to identify membrane proteins, which are often undetectable when using 2D electrophoresis. The majority of these membrane proteins were identified following 1D electrophoresis. Surprisingly, however, some of them were identified by 2D electrophoresis, such as the vomeronasal type-1 receptor A12. Vomeronasal receptors are GPCRs that bind pheromones and are responsible for various behavioral and neuroendocrine responses between individuals (54). Heterodimerization between this vomeronasal receptor and the melatonin MT_1 receptor remains to be demonstrated. The number of identified proteins interacting with the MT_2 C-tail was lesser than that of MT_1. However, several interesting proteins were identified, including catenin δ-1, also known as p120-catenin. This protein is a regulator of cadherin stability and an important modulator of Rho GTPase activities (55). δ-Catenin was first identified through its interaction with presenilin-1, the molecule most frequently mutated in familial Alzheimer disease (56), and shown to interact with mGluR1 receptors by co-immunoprecipitation experiments using rat brain homogenates and dissociate from mGluR1 upon activation by L-glutamate (57).

Approaches based on isolated GPCR subdomains, such as the C-tail, have to be compared with the recently described TAP approach that uses the entire receptor as bait to pull down GPCR-associated protein complexes (24). A careful analysis of the advantages and drawbacks shows that both approaches are rather complementary than mutually exclusive. Whereas the entire receptor allows the purification of protein complexes formed in intact cells, the C-tail approach is more easily accessible for comparing the interactomes of different tissues and under different experimental conditions (different pathophysiological models and pharmacological treatments). A complete list of advantages and drawbacks of both approaches is presented in supplemental Table 2. In contrast to the TAP approach, which is, by itself, a co-immunoprecipitation performed from living cells, interactions between the bait and the proteins identified by approaches using GPCR subdomains need to be confirmed in intact cells with the full-length receptor ideally expressed endogenously. In this study, we validated the interaction between the MT_1 receptor and RGSZ1, a brain-specific protein that belongs to the RGS family (26, 58, 59). RGS proteins have been described as signaling modulators of heterotrimeric $G\alpha$ proteins that increase their rate of GTP hydrolysis and terminate signaling (60–62) and more recently as proteins able to directly interact with GPCRs (27, 63–65). We succeeded in confirming the interaction between the MT_1 receptors and RGSZ1 in cells from the ovine pars tuberalis, which expresses both proteins endogenously, and in transfected HEK 293 cells. The interaction was functional, constitutive, occurred at the plasma membrane, and was only detected with MT_1 but not with MT_2. The constitutive nature of the interaction suggests precoupling of RGSZ1 to MT_1 at the basal state and molecular rearrangement within this pre-existing complex upon agonist stimulation. This model is in good agreement with results described for other RGS proteins (27, 50, 63).

In conclusion, we present here a generic strategy that represents a major methodological advance for the identification of components of GPCR C-tail-associated complexes and overcomes the limitations of currently used genetics and proteomics approaches. Moreover this approach appears to be complementary to recently developed proteomics approaches based on the use of the entire GPCR as bait. Features of this new strategy are the use of chemically synthesized His_6-tagged baits and IMAC that resulted in low nonspecific binding, pH conditions that preserved the integrity of associated protein complexes, and the association of 1D and 2D gel electrophoresis for protein separation that increases the number of identified interaction partners. These 62 candidates will now provide a basis for future cellular studies. Our approach represents a new opportunity for the study of protein complexes associated with GPCRs that can be used to compare GPCR interactomes from different tissues and can be extended to the identification of GPCR-associated complexes under pathological conditions or after *in vivo* pharmacological treatments. Several interactions strongly depend on reversible post-translational modifications such as phosphorylation. *In vitro* phosphorylation of the serine, threonine, and tyrosine residues of GPCR subdomains or the replacement of these residues by phosphomimetic amino acids are two further extensions of our approach to specifically retain those complexes whose interaction depends on receptor phosphorylation.

Acknowledgments—We thank Drs. Martine Migaud and Benoît Malpaux (Institut National de la Recherche Agronomique, Nouzilly, France) for providing pars tuberalis tissue samples, Patty Chen for comments on the manuscript, and Dr. François Guillonneau (both from the Institut Cochin, Paris, France) for invaluable advices.

* This work was supported in part by grants from SERVIER, the Fondation Recherche Médicale ("Equipe FRM"), Fondation pour la Recherche sur le Cerveau (FRC) Neurodon, INSERM, and CNRS. The costs of publication of this article were defrayed in part by the payment of page charges. This article must therefore be hereby marked "*advertisement*" in accordance with 18 U.S.C. Section 1734 solely to indicate this fact.

S The on-line version of this article (available at http://www.mcponline.org) contains supplemental material.

¶ Holds a EGID fellowship.

‡‡ To whom correspondence should be addressed. Tel.: 331-40-51-64-34; Fax: 331-40-51-64-30; E-mail: ralf.jockers@inserm.fr.

REFERENCES

1. Fredriksson, R., Lagerstrom, M. C., Lundin, L. G., and Schioth, H. B. (2003) The G-protein-coupled receptors in the human genome form five main families. Phylogenetic analysis, paralogon groups, and fingerprints. *Mol. Pharmacol.* **63,** 1256–1272
2. Vassilatis, D. K., Hohmann, J. G., Zeng, H., Li, F., Ranchalis, J. E., Mortrud, M. T., Brown, A., Rodriguez, S. S., Weller, J. R., Wright, A. C., Bergmann,

J. E., and Gaitanaris, G. A. (2003) The G protein-coupled receptor repertoires of human and mouse. *Proc. Natl. Acad. Sci. U. S. A.* **100,** 4903–4908
3. Ellis, C., and The *Nature Reviews Drug Discovery* GPCR Questionnaire Participants (2004) The state of GPCR research in 2004. *Nat. Rev. Drug Discov.* **3,** 575, 577–626
4. Milligan, G., and White, J. H. (2001) Protein-protein interactions at G-protein-coupled receptors. *Trends Pharmacol. Sci.* **22,** 513–518
5. Dev, K. K., Nakanishi, S., and Henley, J. M. (2001) Regulation of $mglu_7$ receptors by proteins that interact with the intracellular C-terminus. *Trends Pharmacol. Sci.* **22,** 355–361
6. El Far, O., and Betz, H. (2002) G-protein-coupled receptors for neurotransmitter amino acids: C-terminal tails, crowded signalosomes. *Biochem. J.* **365,** 329–336
7. Bockaert, J., Marin, P., Dumuis, A., and Fagni, L. (2003) The 'magic tail' of G protein-coupled receptors: an anchorage for functional protein networks. *FEBS Lett.* **546,** 65–72
8. Diviani, D., Lattion, A. L., Abuin, L., Staub, O., and Cotecchia, S. (2003) The adaptor complex 2 directly interacts with the α1b-adrenergic receptor and plays a role in receptor endocytosis. *J. Biol. Chem.* **278,** 19331–19340
9. Chen, Z., Hague, C., Hall, R. A., and Minneman, K. P. (2006) Syntrophins regulate α1D-adrenergic receptors through a PDZ domain-mediated interaction. *J. Biol. Chem.* **281,** 12414–12420
10. De Martelaere, K., Lintermans, B., Haegeman, G., and Vanhoenacker, P. (2007) Novel interaction between the human 5-HT7 receptor isoforms and PLAC-24/eIF3k. *Cell. Signal.* **19,** 278–288
11. Bécamel, C., Alonso, G., Galéotti, N., Demey, E., Jouin, P., Ullmer, C., Dumuis, A., Bockaert, J., and Marin, P. (2002) Synaptic multiprotein complexes associated with $5\text{-}HT_{2C}$ receptors: a proteomic approach. *EMBO J.* **21,** 2332–2342
12. Bécamel, C., Gavarini, S., Chanrion, B., Alonso, G., Galéotti, N., Dumuis, A., Bockaert, J., and Marin, P. (2004) The serotonin 5-HT2A and 5-HT2C receptors interact with specific sets of PDZ proteins. *J. Biol. Chem.* **279,** 20257–20266
13. Joubert, L., Hanson, B., Barthet, G., Sebben, M., Claeysen, S., Hong, W., Marin, P., Dumuis, A., and Bockaert, J. (2004) New sorting nexin (SNX27) and NHERF specifically interact with the 5-HT4a receptor splice variant: roles in receptor targeting. *J. Cell Sci.* **117,** 5367–5379
14. Rabilloud, T., and Charmont, S. (2000) Detection of proteins on two-dimensional electrophoresis gels, in *Proteome Research: Two-dimensional Electrophoresis and Identification Methods* (Rabilloud, T., ed) pp. 107–126, Springer, Berlin
15. Gharahdaghi, F., Weinberg, C. R., Meagher, D. A., Imai, B. S., and Mische, S. M. (1999) Mass spectrometric identification of proteins from silver-stained polyacrylamide gel: a method for the removal of silver ions to enhance sensitivity. *Electrophoresis* **20,** 601–605
16. Levoye, A., Dam, J., Ayoub, M. A., Guillaume, J. L., Couturier, C., Delagrange, P., and Jockers, R. (2006) The orphan GPR50 receptor specifically inhibits MT1 melatonin receptor function through heterodimerization. *EMBO J.* **25,** 3012–3023
17. Jockers, R., Da Silva, A., Strosberg, A. D., Bouvier, M., and Marullo, S. (1996) New molecular and structural determinants involved in β2-adrenergic receptor desensitization and sequestration. Delineation using chimeric β3/β2-adrenergic receptors. *J. Biol. Chem.* **271,** 9355–9362
18. Husi, H., Ward, M. A., Choudhary, J. S., Blackstock, W. P., and Grant, S. G. (2000) Proteomic analysis of NMDA receptor-adhesion protein signaling complexes. *Nat. Neurosci.* **3,** 661–669
19. Becamel, C., Figge, A., Poliak, S., Dumuis, A., Peles, E., Bockaert, J., Lubbert, H., and Ullmer, C. (2001) Interaction of serotonin 5-hydroxytryptamine type 2C receptors with PDZ10 of the multi-PDZ domain protein MUPP1. *J. Biol. Chem.* **276,** 12974–12982
20. Stricker, N. L., Christopherson, K. S., Yi, B. A., Schatz, P. J., Raab, R. W., Dawes, G., Bassett, D. E., Bredt, D. S., and Li, M. (1997) PDZ domain of neuronal nitric oxide synthase recognizes novel C-terminal peptide sequences. *Nat. Biotechnol.* **15,** 336–342
21. Ribas, C., Penela, P., Murga, C., Salcedo, A., García-Hoz, C., Jurado-Pueyo, M., Aymerich, I., and Mayor, F., Jr. (2007) The G protein-coupled receptor kinase (GRK) interactome: role of GRKs in GPCR regulation and signaling. *Biochim. Biophys. Acta* **1768,** 913–922
22. Barrett, P., MacLean, A., and Morgan, P. J. (1994) Evidence for multiple forms of melatonin receptor-G-protein complexes by solubilization and gel electrophoresis. *J. Neuroendocrinol.* **6,** 509–515
23. Brydon, L., Roka, F., Petit, L., deCoppet, P., Tissot, M., Barrett, P., Morgan, P. J., Nanoff, C., Strosberg, A. D., and Jockers, R. (1999) Dual signaling of human Mel1a melatonin receptors via Gi2, Gi3, and Gq/11 proteins. *Mol. Endocrinol.* **13,** 2025–2038
24. Daulat, A. M., Maurice, P., Froment, C., Guillaume, J. L., Broussard, C., Monsarrat, B., Delagrange, P., and Jockers, R. (2007) Purification and identification of G protein-coupled receptor protein complexes under native conditions. *Mol. Cell. Proteomics* **6,** 835–844
25. Soares, L., Seroogy, C., Skrenta, H., Anandasabapathy, N., Lovelace, P., Chung, C. D., Engleman, E., and Fathman, C. G. (2004) Two isoforms of otubain 1 regulate T cell anergy via GRAIL. *Nat. Immunol.* **5,** 45–54
26. Wang, J., Ducret, A., Tu, Y., Kozasa, T., Aebersold, R., and Ross, E. M. (1998) RGSZ1, a Gz-selective RGS protein in brain. Structure, membrane association, regulation by Gαz phosphorylation, and relationship to a Gz GTPase-activating protein subfamily. *J. Biol. Chem.* **273,** 26014–26025
27. Bernstein, L. S., Ramineni, S., Hague, C., Cladman, W., Chidiac, P., Levey, A. I., and Hepler, J. R. (2004) RGS2 binds directly and selectively to the M1 muscarinic acetylcholine receptor third intracellular loop to modulate Gq/11α signaling. *J. Biol. Chem.* **279,** 21248–21256
28. Benians, A., Nobles, M., Hosny, S., and Tinker, A. (2005) Regulators of G-protein signaling form a quaternary complex with the agonist, receptor, and G-protein. A novel explanation for the acceleration of signaling activation kinetics. *J. Biol. Chem.* **280,** 13383–13394
29. Abramow-Newerly, M., Roy, A. A., Nunn, C., and Chidiac, P. (2006) RGS proteins have a signalling complex: interactions between RGS proteins and GPCRs, effectors, and auxiliary proteins. *Cell. Signal.* **18,** 579–591
30. Neitzel, K. L., and Hepler, J. R. (2006) Cellular mechanisms that determine selective RGS protein regulation of G protein-coupled receptor signaling. *Semin. Cell Dev. Biol.* **17,** 383–389
31. Zhong, H., Wade, S. M., Woolf, P. J., Linderman, J. J., Traynor, J. R., and Neubig, R. R. (2003) A spatial focusing model for G protein signals. Regulator of G protein signaling (RGS) protein-mediated kinetic scaffolding. *J. Biol. Chem.* **278,** 7278–7284
32. Barrett, P., MacLean, A., Davidson, G., and Morgan, P. J. (1996) Regulation of the Mel 1a melatonin receptor mRNA and protein levels in the ovine pars tuberalis: evidence for a cyclic adenosine 3′,5′-monophosphate-independent Mel 1a receptor coupling and an autoregulatory mechanism of expression. *Mol. Endocrinol.* **10,** 892–902
33. Morgan, P. J. (2000) The pars tuberalis: the missing link in the photoperiodic regulation of prolactin secretion? *J. Neuroendocrinol.* **12,** 287–295
34. Bockaert, J., Fagni, L., Dumuis, A., and Marin, P. (2004) GPCR interacting proteins (GIP). *Pharmacol. Ther.* **103,** 203–221
35. Pluder, F., Mörl, K., and Beck-Sickinger, A. G. (2006) Proteome analysis to study signal transduction of G protein-coupled receptors. *Pharmacol. Ther.* **112,** 1–11
36. Farr, C. D., Gafken, P. R., Norbeck, A. D., Doneanu, C. E., Stapels, M. D., Barofsky, D. F., Minami, M., and Saugstad, J. A. (2004) Proteomic analysis of native metabotropic glutamate receptor 5 protein complexes reveals novel molecular constituents. *J. Neurochem.* **91,** 438–450
37. Ducruet, A. P., Vogt, A., Wipf, P., and Lazo, J. S. (2005) Dual specificity protein phosphatases: therapeutic targets for cancer and Alzheimer's disease. *Annu. Rev. Pharmacol. Toxicol.* **45,** 725–750
38. Torrecilla, I., Spragg, E. J., Poulin, B., McWilliams, P. J., Mistry, S. C., Blaukat, A., and Tobin, A. B. (2007) Phosphorylation and regulation of a G protein-coupled receptor by protein kinase CK2. *J. Cell Biol.* **177,** 127–137
39. Hanyaloglu, A. C., Vrecl, M., Kroeger, K. M., Miles, L. E., Qian, H., Thomas, W. G., and Eidne, K. A. (2001) Casein kinase II sites in the intracellular C-terminal domain of the thyrotropin-releasing hormone receptor and chimeric gonadotropin-releasing hormone receptors contribute to β-arrestin-dependent internalization. *J. Biol. Chem.* **276,** 18066–18074
40. Hirai, T., Niino, Y. S., and Chida, K. (2003) PKCζII, a small molecule of protein kinase C ζ, specifically expressed in the mouse brain. *Neurosci. Lett.* **348,** 151–154
41. McKean, P. G., Vaughan, S., and Gull, K. (2001) The extended tubulin superfamily. *J. Cell Sci.* **114,** 2723–2733
42. Saugstad, J. A., Yang, S., Pohl, J., Hall, R. A., and Conn, P. J. (2002) Interaction between metabotropic glutamate receptor 7 and alpha tubulin. *J. Neurochem.* **80,** 980–988

43. Ciruela, F., Robbins, M. J., Willis, A. C., and McIlhinney, R. A. (1999) Interactions of the C terminus of metabotropic glutamate receptor type 1alpha with rat brain proteins: evidence for a direct interaction with tubulin. *J. Neurochem.* **72,** 346–354
44. Enz, R. (2007) The trick of the tail: protein-protein interactions of metabotropic glutamate receptors. *BioEssays* **29,** 60–73
45. Jarzynka, M. J., Passey, D. K., Ignatius, P. F., Melan, M. A., Radio, N. M., Jockers, R., Rasenick, M. M., Brydon, L., and Witt-Enderby, P. A. (2006) Modulation of melatonin receptors and G-protein function by microtubules. *J. Pineal Res.* **41,** 324–336
46. Janssens, V., and Goris, J. (2001) Protein phosphatase 2A: a highly regulated family of serine/threonine phosphatases implicated in cell growth and signalling. *Biochem. J.* **353,** 417–439
47. Chan, S. F., and Sucher, N. J. (2001) An NMDA receptor signaling complex with protein phosphatase 2A. *J. Neurosci.* **21,** 7985–7992
48. Mao, L., Yang, L., Arora, A., Choe, E. S., Zhang, G., Liu, Z., Fibuch, E. E., and Wang, J. Q. (2005) Role of protein phosphatase 2A in mGluR5-regulated MEK/ERK phosphorylation in neurons. *J. Biol. Chem.* **280,** 12602–12610
49. Guillaume, J. L., Daulat, A. M., Maurice, P., Levoye, A., Migaud, M., Brydon, L., Malpaux, B., Borg-Capra, C., and Jockers, R. (2008) The PDZ protein MUPP1 promotes G_i coupling and signalling of the MT_1 melatonin receptor. *J. Biol. Chem.* **283,** 16762–16771
50. Roy, A. A., Lemberg, K. E., and Chidiac, P. (2003) Recruitment of RGS2 and RGS4 to the plasma membrane by G proteins and receptors reflects functional interactions. *Mol. Pharmacol.* **64,** 587–593
51. Kim, E., and Sheng, M. (2004) PDZ domain proteins of synapses. *Nat. Rev. Neurosci.* **5,** 771–781
52. Christenn, M., Kindler, S., Schulz, S., Buck, F., Richter, D., and Kreienkamp, H. J. (2007) Interaction of brain somatostatin receptors with the PDZ domains of PSD-95. *FEBS Lett.* **581,** 5173–5177
53. Zhang, J., Vinuela, A., Neely, M. H., Hallett, P. J., Grant, S. G., Miller, G. M., Isacson, O., Caron, M. G., and Yao, W. D. (2007) Inhibition of the dopamine D1 receptor signaling by PSD-95. *J. Biol. Chem.* **282,** 15778–15789
54. Rouquier, S., and Giorgi, D. (2006) Olfactory receptor gene repertoires in mammals. *Mutat. Res.* **616,** 95–102
55. Reynolds, A. B. (2007) p120-catenin: past and present. *Biochim. Biophys. Acta* **1773,** 2–7
56. Zhou, J., Liyanage, U., Medina, M., Ho, C., Simmons, A. D., Lovett, M., and Kosik, K. S. (1997) Presenilin 1 interaction in the brain with a novel member of the Armadillo family. *Neuroreport* **8,** 2085–2090
57. Jones, S. B., Lanford, G. W., Chen, Y. H., Morabito, M., Moribito, M., Kim, K., and Lu, Q. (2002) Glutamate-induced δ-catenin redistribution and dissociation from postsynaptic receptor complexes. *Neuroscience* **115,** 1009–1021
58. Glick, J. L., Meigs, T. E., Miron, A., and Casey, P. J. (1998) RGSZ1, a Gz-selective regulator of G protein signaling whose action is sensitive to the phosphorylation state of Gzα. *J. Biol. Chem.* **273,** 26008–26013
59. Larminie, C., Murdock, P., Walhin, J. P., Duckworth, M., Blumer, K. J., Scheideler, M. A., and Garnier, M. (2004) Selective expression of regulators of G-protein signaling (RGS) in the human central nervous system. *Brain Res. Mol. Brain Res.* **122,** 24–34
60. Ross, E. M., and Wilkie, T. M. (2000) GTPase-activating proteins for heterotrimeric G proteins: regulators of G protein signaling (RGS) and RGS-like proteins. *Annu. Rev. Biochem.* **69,** 795–827
61. Hollinger, S., and Hepler, J. R. (2000) Cellular regulation of RGS proteins: modulators and integrators of G protein signaling. *Pharmacol. Rev.* **54,** 527–559
62. Willars, G. B. (2006) Mammalian RGS proteins: multifunctional regulators of cellular signalling. *Semin. Cell Dev. Biol.* **17,** 363–376
63. Hague, C., Bernstein, L. S., Ramineni, S., Chen, Z., Minneman, K. P., and Hepler, J. R. (2005) Selective inhibition of α1A-adrenergic receptor signaling by RGS2 association with the receptor third intracellular loop. *J. Biol. Chem.* **280,** 27289–27295
64. Georgoussi, Z., Leontiadis, L., Mazarakou, G., Merkouris, M., Hyde, K., and Hamm, H. (2006) Selective interactions between G protein subunits and RGS4 with the C-terminal domains of the μ- and δ-opioid receptors regulate opioid receptor signaling. *Cell. Signal.* **18,** 771–782
65. Snow, B. E., Hall, R. A., Krumins, A. M., Brothers, G. M., Bouchard, D., Brothers, C. A., Chung, S., Mangion, J., Gilman, A. G., Lefkowitz, R. J., and Siderovski, D. P. (1998) GTPase activating specificity of RGS12 and binding specificity of an alternatively spliced PDZ (PSD-95/Dlg/ZO-1) domain. *J. Biol. Chem.* **273,** 17749–17755